Nano Research

Open Access

Research Article

Processable subnanowire-liquid crystal ink for encryption and anti-counterfeiting

Jiangxiao Li[1], Wenxiong Shi[2], Shange Qi[1], Shuai Lin[1], Simin Zhang[1]✉, and Xun Wang[3]✉

[1] *School of Chemistry and Chemical Engineering, Beijing Institution of Technology, Beijing 100081, China*
[2] *Institute for New Energy Materials and Low Carbon Technologies, School of Materials Science and Engineering, Tianjin University of Technology, Tianjin 300384, China*
[3] *Lab of Organic Optoelectronics and Molecular Engineering, Department of Chemistry, Tsinghua University, Beijing 100084, China*

Cite this article: *Nano Research*, **2025**, *18*, 94907334. https://doi.org/10.26599/NR.2025.94907334

ABSTRACT: Information encrypting and anti-counterfeiting have attracted increasing attention in the fields of information communications and Internet of Things. It is of great significance to construct advanced stimuli-responsive materials with simple encryption/decryption procedures and high reliability. Herein, the subnanowire (SNW)-liquid crystal (LC) ink was prepared with Bi_2O_3-PMoO SNWs and commercial LCs 4'-pentyl-[1,1'-biphenyl]-4-carbonitrile (5CB), which can be used for preparing films and patterning through blade coating or writing/printing. Through combining photothermal conversion performance of SNWs with thermotropic phase transition of LCs and smart design and patterning, different forms of SNW-LC materials with photoresponsive performance can be applied in multiple-mode information encryption and anti-counterfeiting effectively, exhibiting fast response rate (within 10 s), high sensitivity (even flashlight of mobile phone), and great stability (over 100 cycles). Considering the versatility and easy processability of SNW-LC ink and the good responsiveness and high reliability of SNW-LC materials, combination of SNWs and LCs may be a potential candidate for effective encryption and anti-counterfeiting.

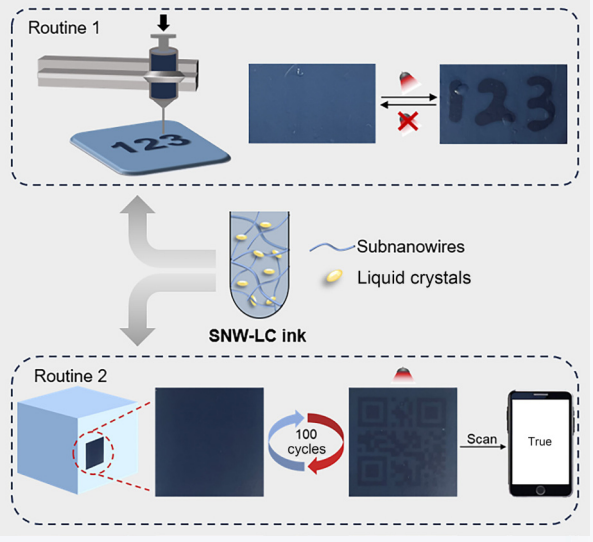

KEYWORDS: subnanowires, liquid crystal, photoresponsive, encryption, anti-counterfeiting

1 Introduction

In modern life, industry, military, and other fields, information security has become increasingly important [1–3]. In order to distinguish false information and prevent information leakage, various advanced materials used for information encryption and anti-counterfeiting technology have been developed, such as fluorescent/phosphorescent materials, photonic crystals, and watermarks. [4–16]. Among them, stimuli-responsive materials attract considerable attention because they need specific stimuli to trigger decryption and thus enhance the security level. Liquid crystals (LCs) exhibit unique molecular mobility and order of molecules [17], and their phase transition [18], color variation [3, 6], and optical effect [19–21] under external fields show great potential in effective information encryption and anti-counterfeiting. LC elastomers (LCEs) [22–27], polymer-stabilized LCs (PSLCs) [28–31], LC nanoparticles [32–34], etc., have been studied extensively due to their response to light, heat, and electric fields. However, achieving convenient and reliable information encryption for practical applications with LCs as the response switch still faces some problems, such as complex molecular design and synthesis, expensive decryption devices, and decay of sensitivity and reliability. It is necessary to develop LCs-based anti-counterfeiting materials with simple preparation method, low cost, high sensitivity, and good stability.

Subnanowires (SNWs) possess diameters of about 1 nm, simultaneously possessing the multi-functions of inorganic

Received: February 14, 2025; **Revised:** February 21, 2025
Accepted: February 25, 2025

✉Address correspondence to Simin Zhang, zhangsimin@bit.edu.cn; Xun Wang, wangxun@mail.tsinghua.edu.cn

nanomaterials and polymer-analogue properties [35, 36]. Firstly, SNWs exhibit various properties depending on the compositions and structures, such as photothermal conversion, catalysis, gelation, fluorescence, photochromism, and photoelectric response. [35, 37–43], which are potential to combine with LCs to achieve multi-level information encryption. In addition, SNWs not only show unique self-assembly characteristics [44–47], forming superlattices, chiral assembles, etc., but also can be processed like polymers; thus, freestanding fibers, films, fabrics, etc., can be obtained successfully [48–51]. Therefore, combining SNWs and LCs may provide a promising approach for constructing effective encryption and anti-counterfeiting materials for broad applications.

In this work, the SNW-LC ink was prepared with Bi_2O_3-PMoO SNWs and commercial LCs 4'-pentyl-[1,1'-biphenyl]-4-carbonitrile (5CB). Firstly, the photoresponsive film was constructed using the SNW-LC ink through a facile blade coating method (Fig. 1(a)). Moreover, the SNW-LC ink can also be patterned by writing/printing conveniently. SNWs and LCs assist each other in assembly, and LCs maintain a certain degree of freedom among SNWs, so molecular motion during the phase transition of LCs is allowed in the SNW-LC materials. Through combining photothermal conversion performance of SNWs and thermotropic phase transition of LCs, the SNW-LC materials exhibit significant change of haze with/without illumination. Thus, the information can be encrypted and decrypted. The SNW-LC materials exhibit fast response rate (within 10 s), high sensitivity (even flashlight of mobile phone), and great stability (over 100 cycles), which is significant in information encryption and anti-counterfeiting. Through smart design and patterning, different forms of SNW-LC materials can be applied in multiple-mode information encrypting and anti-counterfeiting effectively.

2 Results and discussion

2.1 Characterizations of SNWs and LCs

Bi_2O_3-PMoO SNWs were prepared according to a previously reported method, and details can be found in experimental section

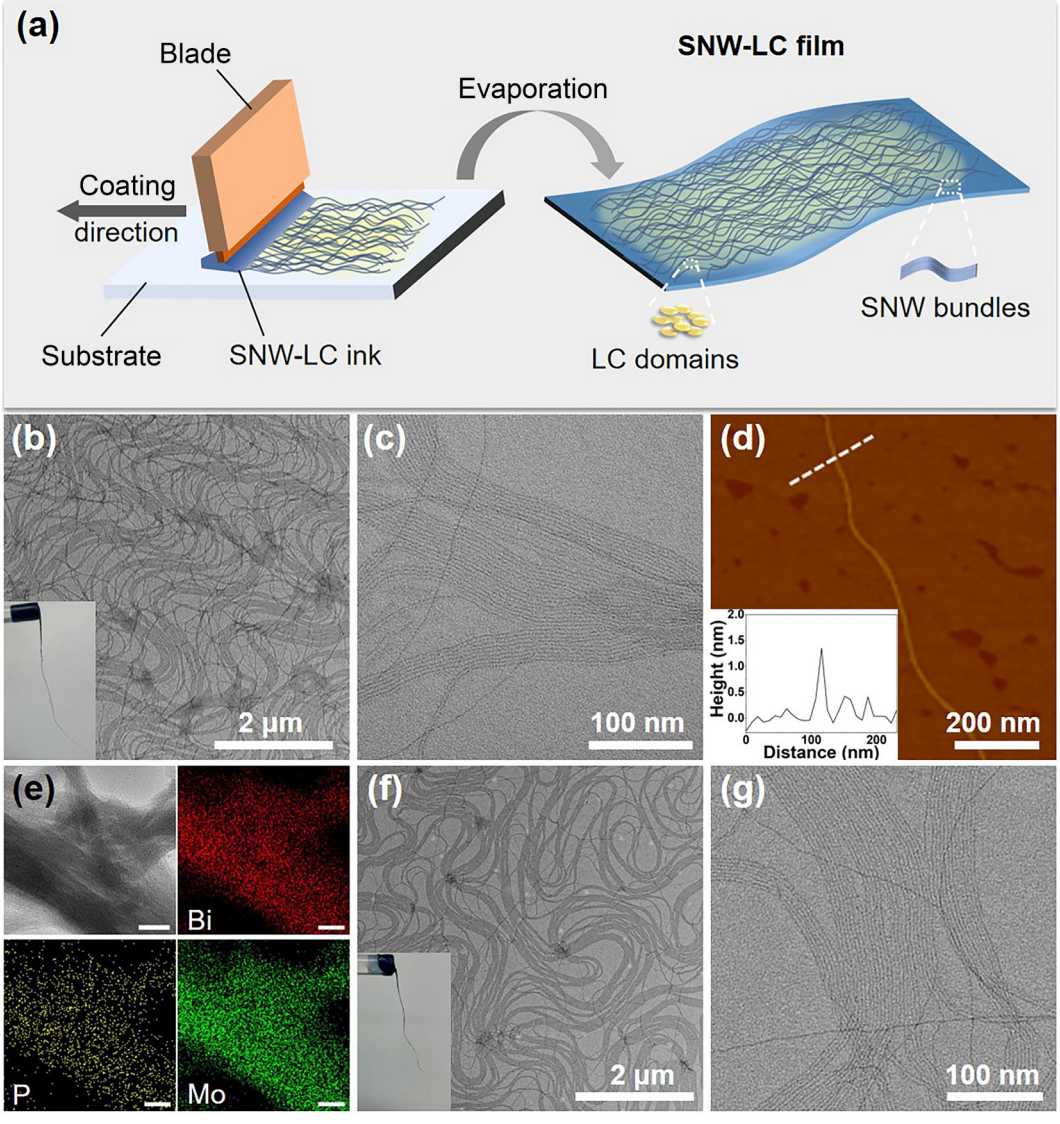

Figure 1 Characterizations of Bi_2O_3-PMoO SNWs and 5CB. (a) Schematic of fabrication and structures of the SNW-LC film. ((b) and (c)) TEM images of SNWs. The inset in (b) is a photograph of the fiber drawn from the dispersion of SNWs. (d) AFM results of the SNW. (e) EDS mapping images of SNWs. Scale bars: 100 nm. ((f) and (g)) TEM images of the SNW-LC ink. The inset in (f) is a photograph of the SNW-LC fiber.

in the Electronic Supplementary Material (ESM). As shown in Fig. 1(b), SNWs at low magnification show a high degree of purity. Flexible SNW fibers can be drawn from the dispersion by a glass rod, demonstrating high viscosity of the dispersion (inset of Fig. 1(b)). As shown in transmission electron microscopy (TEM) and atomic force microscopy (AFM) results, SNWs are arranged neatly (Fig. 1(c)), and the diameter of a single SNW is approximately 1 nm (Fig. 1(d)). The energy-dispersive spectroscopy (EDS) mapping analysis (Fig. 1(e)) and the X-ray photoelectron spectroscopy (XPS) (Fig. S1 in the ESM) confirmed that the prepared SNWs are composed of bismuth oxide and phosphomolybdic acid and they distribute uniformly along SNWs. Bi_2O_3-PMoO SNWs show good photothermal conversion performance, and 5CB shows thermotropic phase transition, so 5CB was introduced into Bi_2O_3-PMoO SNWs to prepare the SNW-LC ink in order to fabricate photoresponsive materials. After introducing 5CB (Fig. S2 in the ESM), SNWs maintain the original morphologies and viscosity (Figs. 1(f) and 1(g)), demonstrating 5CB shows no damage to SNWs.

2.2 Characterizations of the SNW-LC film

The SNW-LC ink was prepared through dispersing Bi_2O_3-PMoO SNWs and 5CB in cyclohexane, exhibiting viscosity and shear thinning properties (Fig. S3 in the ESM). The freestanding SNW-LC film was successfully constructed with the SNW-LC ink through the facile blade coating method (Fig. 1(a) and Fig. S4 in the ESM). As shown in Fig. 2(a), a square SNW-LC film was prepared on a glass plate. The freestanding film can bend and curl without damage, showing remarkable flexibility (Figs. 2(b) and 2(c)). After 1000 times bending cycles, the SNW-LC films do not show any crack and wrinkle, and the tensile strength is basically the same as before the cyclic bending test (Fig. S5 in the ESM). As shown in scanning electron microscopy (SEM) image (Fig. S6 in the ESM), the SNW-LC film shows a smooth surface and no obvious defect. The thickness of the film is about 22 μm, and it shows a layered structure (Fig. S7 in the ESM). Meanwhile, the water contact angle (CA) with the film is 100.2° (Fig. 2(d)), proving the SNW-LC film is hydrophobic. As shown in the stress–strain curves (Fig. 2(e)), the pure SNW film and SNW-LC film show fracture stresses of 5.8 and 4.0 MPa, respectively, and the elongation break of them are 1.1% and 4.6%, respectively. Compared to the pure SNW film, the SNW-LC film exhibits better flexibility and deformability. This is because that LCs play a role like plasticizers, increasing the free volume and the lubricity among SNWs. As shown in the small-angle X-ray diffraction (SAXRD) patterns (Fig. 2(f)), the peak of the SNW-LC film shows stronger peak and lower θ value of the peak position than the pure SNW film, suggesting LCs fill in interspacing between SNWs and assist them to arrange into the more ordered structure.

The molecular dynamic (MD) simulation was conducted to investigate the interaction between SNWs and LCs and structures of the LC-SNW film. Upon introducing one SNW and twelve 5CB into the system, the corresponding model diagram along the *z*-axis (Fig. 2(g)) exhibits an internal order. 5CB interacts with SNWs through cyano groups, which is closer to SNWs, indicating 5CB and SNWs assist each other in assembly. When numerous of 5CB molecules are introduced, it becomes evident that LCs not only absorb onto the SNWs surfaces but also occupy the interstitial spaces between adjacent SNWs (Figs. S8(a)–S8(d) in the ESM). During the simulation process, as 5CB and SNWs contact with each other through van der Waals and electrostatic forces and finally reach a state of equilibrium (Fig. S8(e) in the ESM), the potential energy of the system decreases initially and subsequently reaches a plateau (Fig. S8(f) in the ESM). While SNWs and LCs co-assemble into an ordered pattern, LCs maintain a certain degree of

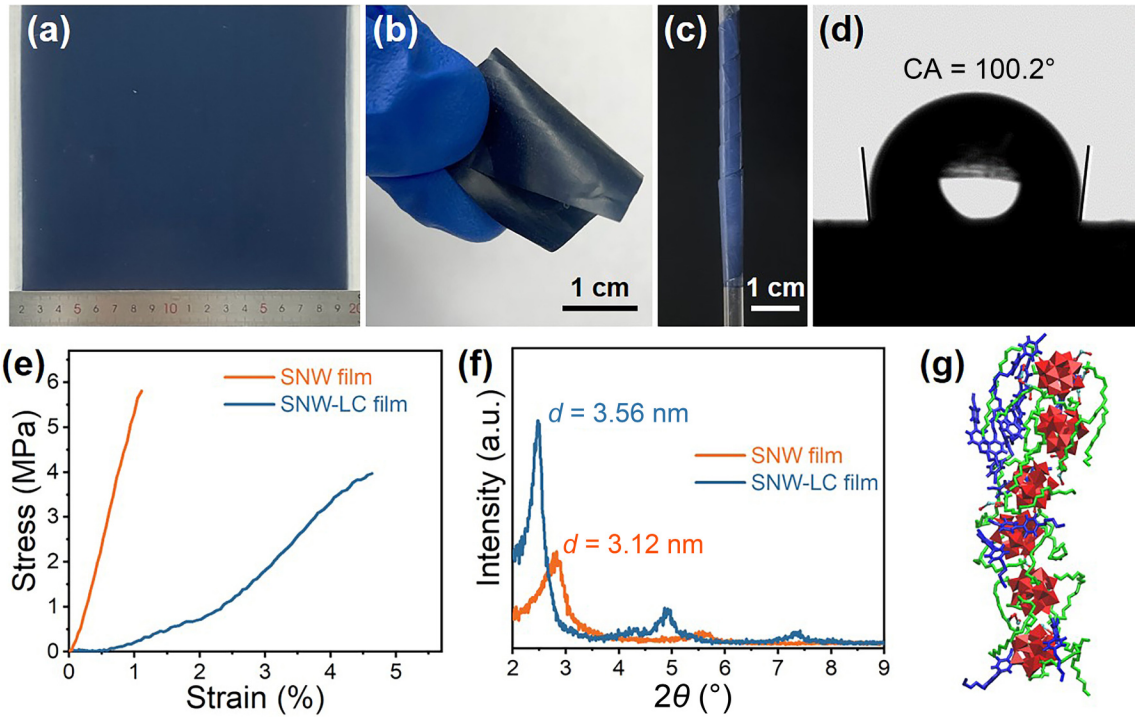

Figure 2 Characterizations of the SNW-LC film. ((a)–(c)) Photographs of the SNW-LC film. (d) The water CA with the SNW-LC film. (e) Tensile stress–strain curves of the SNW film and SNW-LC film. (f) SAXRD patterns of the SNW film and SNW-LC film. (g) The corresponding model diagram along the *z*-axis obtained by MD simulation. The red tetrahedron represents phosphomolybdic acid clusters, and green chain structure represents the oleylamine. The cyan and red balls represent bismuth and oxygen atoms, respectively. The blue molecule represents 5CB.

freedom simultaneously, so molecular motion during the phase transition of LCs is allowed in the freestanding SNW-LC film.

2.3 Photoresponsive performance of the SNW-LC film

The SNW-LC film shows good photoresponsivity, even when illuminated by flashlight of mobile phone; the transparency of the SNW-LC film can increase obviously (Fig. 3(a) and Movie S1 in the ESM). As shown in Figs. 3(b) and 3(c), the SNW-LC film with 30 wt.% 5CB and the thickness of 22 μm shows good photothermal performance and stability. As shown in Fig. 3(b), the temperature of the SNW-LC film increases to 50 °C (surpassing the phase transition temperature of 5CB, 35.5 °C) within 10 s, meaning fast photoresponsive rate. After 5 cycles of photothermal conversion, there is no degradation of performance (Fig. 3(c)), demonstrating good photoresponsive stability. The ultraviolet–visible (UV–vis) absorption spectra of the pure SNW film and SNW-LC film show no significant difference, indicating the absorbance has negligible influence on transparency of the SNW-LC film (Fig. 3(d)). Furthermore, the scattering ability of the SNW-LC film was tested (Figs. 4(a) and 4(b)). When illuminated with xenon lamp, the scattering ability of the SNW-LC film decreases, and the forward scattered light is more concentrated, and the light spot is brighter. Without illumination, the incident light is severely scattered, and the scattered light spot is almost indistinguishable. According to the above results, the haze change is the main reason for the transparency change of the SNW-LC film. As shown in Fig. S9 in the ESM, the pure Bi_2O_3-PMoO SNW film, pure 5CB, and GdOOH SNW-LC film have no photoresponsive performance, indicating the necessity of synergistic effect between Bi_2O_3-PMoO SNWs and LCs.

Bi_2O_3-PMoO SNWs provide the photothermal conversion performance, and LCs provide the thermotropic phase transition. Under light illumination, the temperature of the SNW-LC film increases. Within 10 s, the temperature of the film can reach the clearing point of 5CB (35.5 °C), causing it to undergo a phase transition. This will weaken its scattering ability, leading to transparency increase in the SNW-LC film. When the light illumination is removed, the temperature of the SNW-LC film decreases. When the temperature drops below the clearing point of 5CB, it will undergo a reverse phase transition, causing the scattering ability to be recovered and leading to a transparency decrease of the SNW-LC film. The content of LCs and thickness of the film have important influence on the performance of the LC-SNW film. Firstly, when the content of LCs is increased, the scattering ability can be enhanced, and the contrast of light spots is more obvious before and after illumination (Fig. 4(c)). However, excessive LCs lead to severe decrease of mechanical properties of the SNW-LC film (Fig. S10 in the ESM) and even cause many defects in the film (Fig. S11 in the ESM). Secondly, when a SNW-LC film is covered on English letters, if the film is too thin, the English letters cannot be concealed before light illumination; if the film is too thick, the English letters cannot be revealed (Fig. 4(d)). Comprehensively considering the scattering ability, mechanical properties, and transparency, the film with 30% 5CB and the thickness of 22 μm is chosen for subsequent applications. The SNW-LC film can response to light fast and adjust itself into "ON" or

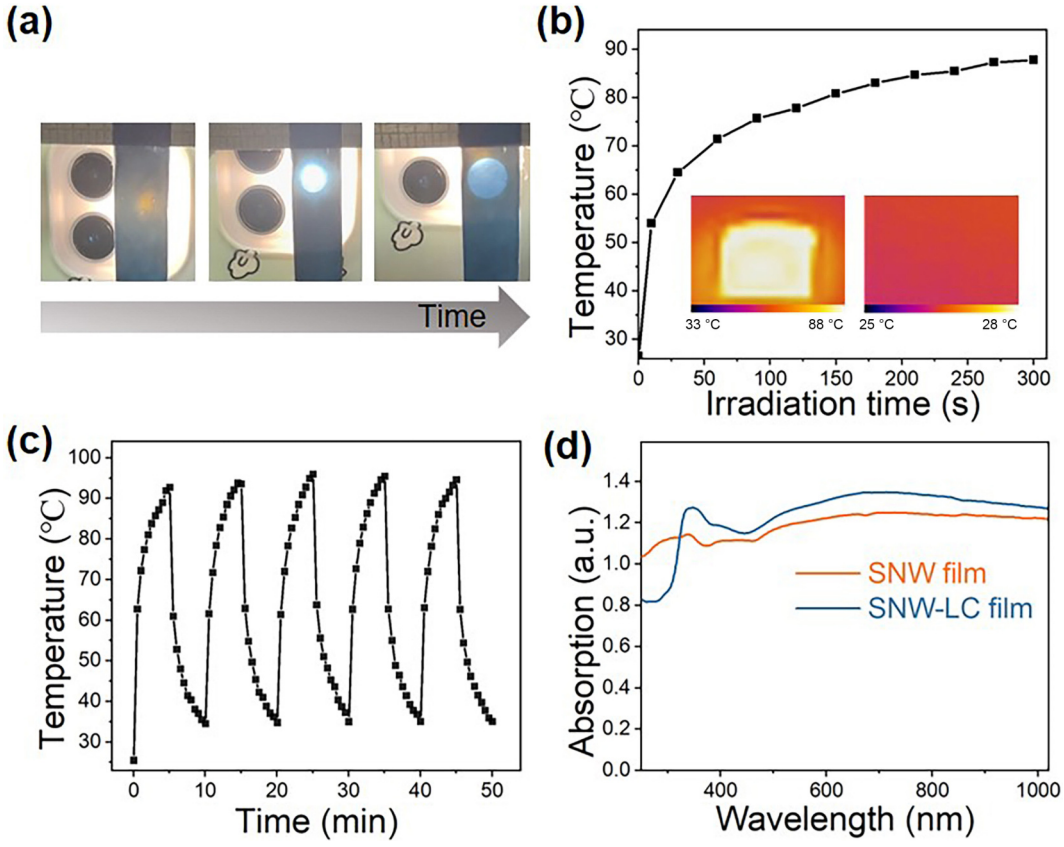

Figure 3 The photoresponsive performance of the SNW-LC film. (a) Photographs of the SNW-LC film illuminated by the flashlight of mobile phone. (b) Photothermal conversion performance of the SNW-LC film. Insets are infrared images of the film before and after illumination. (c) Photothermal stability of the SNW-LC film during 5 cycles. The above photothermal performance is measured with a xenon lamp (0.3 W·cm^{-2}). (d) UV–vis absorption spectra of films.

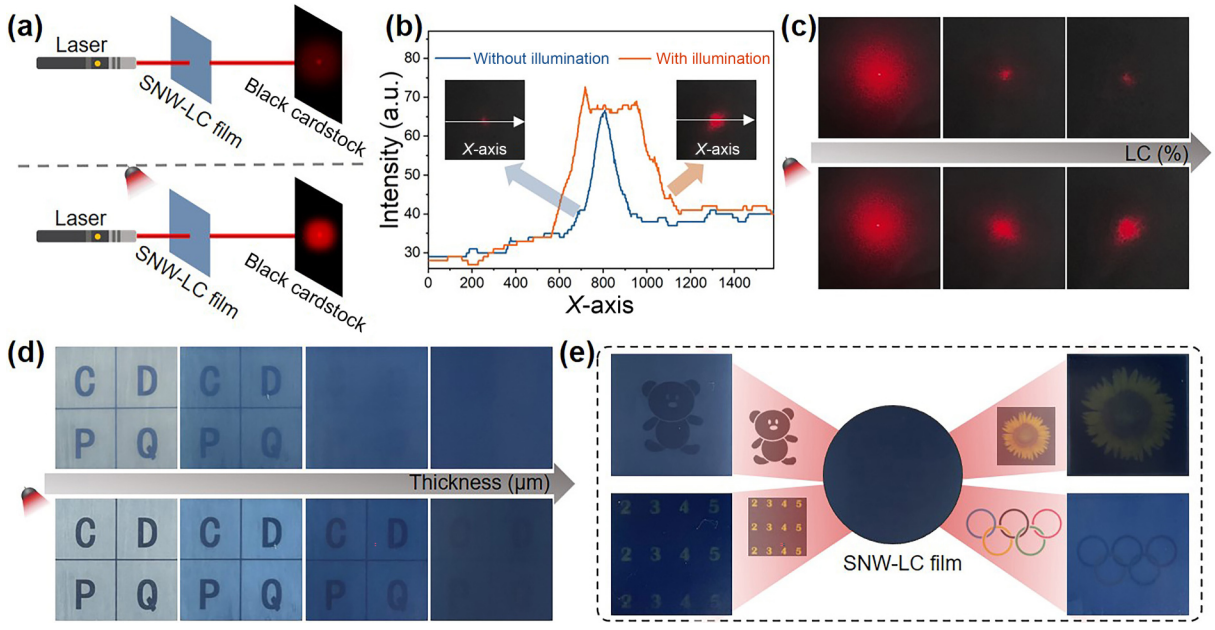

Figure 4 The optimization of the SNW-LC film with photoresponsive performance. (a) The schematic diagram of scattering ability test of SNW-LC film. (b) The light intensity along the *x*-axis through the scatter light spot of SNW-LC film before and after illumination. The above thickness of tested film is 22 μm, and the 5CB content is 30 wt.%. (c) Forward scatter light spots of SNW-LC films (22 μm, with 0 wt.%, 15 wt.%, and 30 wt.% 5CB content, respectively) before (top) and after (bottom) illumination. (d) Photographs of SNW-LC films with different thicknesses (8, 15, 22, and 29 μm, 30 wt.% of 5CB) covered on English letters before (top) and after (bottom) illumination. (e) Photographs of SNW-LC films (22 μm, 30 wt.% of 5CB) covered on different patterns before (top) and after (bottom) illumination. Samples are illuminated by a xenon lamp (0.3 W·cm^{-2}) for 10 s.

"OFF" state. This photoresponsive characteristic renders the SNW-LC film promising for potential applications in information encrypting and anti-counterfeiting. As shown in Fig. 4(e), the SNW-LC film is covered in different patterns, and this information will be encrypted. When under light illumination, the information will be decrypted. The photothermal function and processability of SNWs are combined with basic thermal phase transition of commercial LCs to fabricate this kind of freestanding and flexible photoresponsive film. The preparation of this SNW-LC film is simple, without complex molecular design and synthesis.

2.4 Applications in information anti-counterfeiting and encryption

The SNW-LC ink and the SNW ink are easily patterned and can be used for writing and printing conveniently, and different forms of SNW-LC materials applied in multiple-mode information encrypting and anti-counterfeiting are explored. As shown in Fig. 5(a), a pure SNW film serves as the paper, where the code "123" is written with the SNW-LC ink since there is little difference in colour between SNW ink and SNW-LC ink. Without illumination, the code is unrecognizable, and after being illuminated, the codes can be decrypted. Through this method, the SNW-LC ink and SNW paper for encrypted writing can be applied in information encryption. As shown in Fig. 5(b), an integrated anti-counterfeiting label is fabricated with the SNW-LC film covering on two-dimensional code, which can be attached to packaging. The two-dimensional code will be damaged at the same time through mechanical damage of the SNW-LC film. Only under light illumination, the two-dimensional code can be revealed. Through scanning with a mobile phone, the information can be decrypted, proving the authenticity of the product. As shown in Fig. 5(c), specific codes are printed with the SNW-LC ink and the SNW ink, which contains true codes (indicated with red dash line) printed with the SNW-LC ink and the other parts are printed with the SNW ink. Under visible light, false information "8888" is shown, and the true code cannot be recognized directly by eye recognition due to low contrast. Under illumination and running the image recognition program (details are shown in the ESM), the true information "7269" can be decrypted. The SNW-LC materials show good photoresponsive stability and reliability after working for multiple cycles, increasing their service life and ensuring durability. SNWs not only play as the substrate, but also are essential for the photoresponsive performance.

3 Conclusion

In summary, through combining the photothermal function and processability of SNWs with basic thermal phase transition of LCs, the SNW-LC ink was prepared, which can be used for constructing film and writing/printing. Through cleverly designing, multiple-mode information encryption and anti-counterfeiting can be achieved by SNW-LC materials. The photoresponsivity of the SNW-LC materials is great, showing fast response rate (within 10 s), high sensitivity (even flashlight of mobile phone), and great stability (over 100 cycles), which is significant in information encryption and anti-counterfeiting. Combining SNWs and LCs provides a new solution for problems of complex molecular design and synthesis, expensive decryption devices, and the decay of sensitivity and reliability in LC-based encryption materials. More importantly, SNWs own various functional properties, such as photothermal conversion, gelation, fluorescence, photochromism, and photoelectric response. Combining SNWs and LCs effectively provides a new way for achieving convenient and reliable information encryption in practical applications.

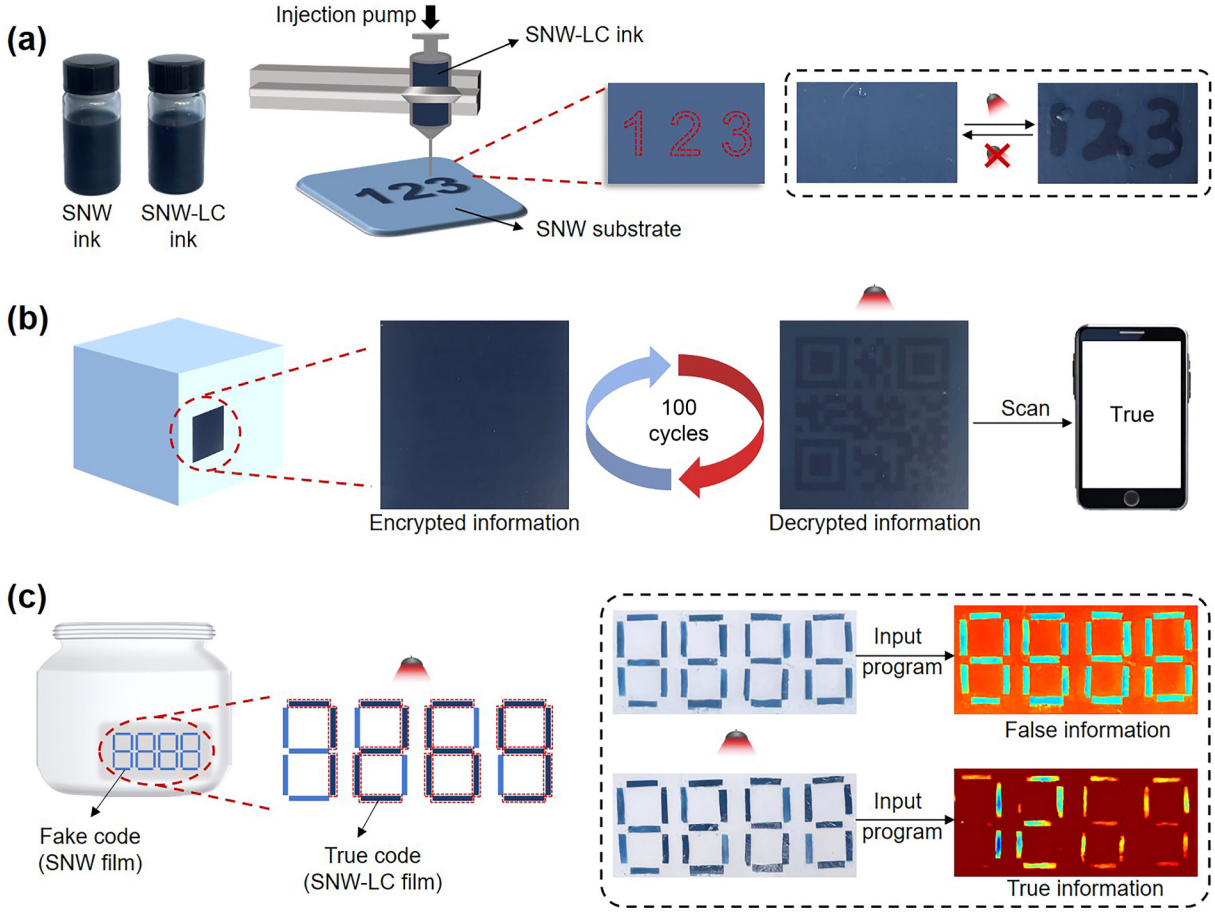

Figure 5 Information encryption and anti-counterfeiting based on photoresponsive SNW-LC materials. (a) The information encryption through writing with the SNW-LC ink on a SNW paper. (b) Anti-counterfeiting labels fabricated with SNW-LC film and two-dimensional code. (c) The information encryption and anti-counterfeiting through printing codes with the SNW-LC ink and the SNW ink. Samples are illuminated by a xenon lamp (0.3 W·cm^{-2}) for 10 s.

Electronic Supplementary Material: Supplementary material (experimental methods, Figs. S1–S11, and Movie S1) is available in the online version of this article at https://doi.org/10.26599/NR.2025.94907334.

Data availability

All data needed to support the conclusions in the paper are presented in the manuscript and the Electronic Supplementary Material. Additional data related to this paper may be requested from the corresponding author upon request.

Acknowledgements

This work was financially supported by Beijing Institute of Technology Teli Young Fellow program, Young Elite Scientist Sponsorship Program by CAST (No. 2022QNRC001), the National Natural Science Foundation of China (NSFC, No. 22375018), and Xiaomi Young Scholar Program. Thanks for Shijiazhuang Chengzhi Yonghua Display Material Co., Ltd. for providing 5CB. We thank Z. L., Y. H., P. H., Analysis & Testing Center of Beijing Institution of Technology, and Tsinghua University Analysis Center for assisting with testing.

Declaration of competing interest

X. W. is the Associate editor of this journal, but he is not involved in the peer-review or decision of this article. The other contributing authors report no conflict of interests in this work.

Author contribution statement

J. X. L.: Writing manuscript, experimental design. W. X. S.: MD simulations. S. G. Q. and S. L.: Assisting experiments. S. M. Z. and X. W.: Guiding research and revising manuscript. All the authors have approved the final manuscript.

Use of AI statement

None.

References

[1] Arppe, R.; Sørensen, T. J. Physical unclonable functions generated through chemical methods for anti-counterfeiting. *Nat. Rev. Chem.* **2017**, *1*, 0031.

[2] Yang, Y. B.; Li, Q. Y.; Zhang, H. W.; Liu, H.; Ji, X. F.; Tang, B. Z. Codes in code: AIE supramolecular adhesive hydrogels store huge amounts of information. *Adv. Mater* **2021**, *33*, 2105418.

[3] Pang, X. K.; Zhang, Q.; Wang, J. Y.; Jiang, X.; Wu, M. L.; Cui, M. Y.; Feng, Z. X.; Xu, W. X.; Song, B.; He, Y. Artificial optical microfingerprints for advanced anti-counterfeiting. *Nano Res.* **2024**, *17*, 4371–4378.

[4] Duan, R.; Tang, R. Q.; Tong, Y. P.; Zhao, D. Y.; Tang, B. Z. Double-

state anticounterfeiting labels based on light-emitting polymer-stabilized blue phase. *Adv. Funct. Mater.* **2023**, *33*, 2306069.
[5] Yang, X. R.; Sheng, Y. H.; Zhang, L. L.; Yang, L.; Xing, F. J.; Di, Y. S.; Liu, C. H.; Hu, F. R.; Yang, X. F.; Yang, G. F. et al. Five-level anti-counterfeiting based on versatile luminescence of tri-doped double perovskites. *Nano Res.* **2024**, *17*, 9971–9979.
[6] Wang, X. J.; Zhao, B.; Deng, J. P. Liquid crystals doped with chiral fluorescent polymer: Multi-color circularly polarized fluorescence and room-temperature phosphorescence with high dissymmetry factor and anti-counterfeiting application. *Adv. Mater.* **2023**, *35*, 2304405.
[7] Zhang, J. Y.; Song, C. J.; Zhang, S. N.; Qin, S. Y.; Ren, Y. X.; Zhang, L. Y.; Xiao, J. M.; Li, K. X.; Hu, W.; Yang, H. Time-dependent information encryption in liquid crystalline polymer with programmable glass transition temperature. *Adv. Funct. Mater.* **2024**, *34*, 2400030.
[8] Guo, X.; Sun, X. N.; Zhang, J. F.; Huang, Y. F.; Liu, X. H.; Liu, X.; Xu, W. L.; Chen, D. Z. Luminescent mechanism and anti-counterfeiting application of hydrophilic, undoped room-temperature phosphorescent silicon nanocrystals. *Small* **2024**, *20*, 2303464.
[9] Liu, Q.; Liu, X. Q.; Yu, X. X.; Zhang, X. H.; Zhu, M. F.; Cheng, Y. H. Circularly polarized room temperature phosphorescence through twisting-induced helical structures from polyvinyl alcohol-based fibers containing hydrogen-bonded dyes. *Angew. Chem., Int. Ed.* **2024**, *63*, e202403391.
[10] Gao, Y. F.; Ge, K. Y.; Zhang, Z.; Li, Z.; Hu, S. W.; Ji, H. J.; Li, M. Y.; Feng, H. H. Fine optimization of colloidal photonic crystal structural color for physically unclonable multiplex encryption and anti-counterfeiting. *Adv. Sci.* **2024**, *11*, 2305876.
[11] Huang, H. W.; Li, H. T.; Yin, J. M.; Gu, K.; Guo, J.; Wang, C. Butterfly-inspired tri-state photonic crystal composite film for multilevel information encryption and anti-counterfeiting. *Adv. Mater.* **2023**, *35*, 2211117.
[12] Ma, W. B.; Da, B. X.; Zheng, G. Q.; Dai, K.; Liu, C. T.; Shen, C. Y. Facile preparation of robust microgrooves based photonic crystals film for anti-counterfeiting. *Polymer* **2023**, *276*, 125889.
[13] Qi, Y.; Zhang, S. F. Recent advances in multifunctional shape memory photonic crystals and practical applications. *Nano Res.* **2024**, *17*, 79–96.
[14] Li, Z. L.; Dai, Q.; Deng, L. G.; Zheng, G. X.; Li, G. F. Structural-color nanoprinting with hidden watermarks. *Opt. Lett.* **2021**, *46*, 480–483.
[15] Jeon, H. J.; Leem, J. W.; Ji, Y.; Park, S. M.; Park, J.; Kim, K. Y.; Kim, S. W.; Kim, Y. L. Cyber-physical watermarking with inkjet edible bioprinting. *Adv. Funct. Mater.* **2022**, *32*, 2112479.
[16] He, Z. H.; Liu, K. X.; Cao, L. C. Watermarking and encryption for holographic communication. *Photonics* **2022**, *9*, 675.
[17] Tschierske, C. Liquid crystal engineering—New complex mesophase structures and their relations to polymer morphologies, nanoscale patterning and crystal engineering. *Chem. Soc. Rev.* **2007**, *36*, 1930–1970.
[18] Gao, Y. Z.; Feng, K.; Zhang, J.; Zhang, L. Y. Finger-temperature-detecting liquid crystal composite film for anti-counterfeiting labels. *Molecules* **2020**, *25*, 521.
[19] Yu, J. S.; Son, H. J.; Kim, J. H. An anti-counterfeit technique using elastic and optical properties of liquid crystals. *Liq. Cryst.* **2023**, *50*, 1617–1623.
[20] Yang, X. F.; Jin, X.; Zheng, A. Y.; Duan, P. F. Dual band-edge enhancing overall performance of upconverted near-infrared circularly polarized luminescence for anticounterfeiting. *ACS Nano* **2023**, *17*, 2661–2668.
[21] Anusuyadevi, P. R.; Shanker, R.; Cui, Y. X.; Riazanova, A. V.; Järn, M.; Jonsson, M. P.; Svagan, A. J. Photoresponsive and polarization-sensitive structural colors from cellulose/liquid crystal nanophotonic structures. *Adv. Mater.* **2021**, *33*, 2101519.
[22] Liu, X. Y.; Wei, R. B.; Hoang, P. T.; Wang, X. G.; Liu, T.; Keller, P. Reversible and rapid laser actuation of liquid crystalline elastomer micropillars with inclusion of gold nanoparticles. *Adv. Funct. Mater.* **2015**, *25*, 3022–3032.
[23] Wang, H. Q.; Tang, Y. Q.; Huang, Z. Y.; Wang, F. Z.; Qiu, P. F.; Zhang, X. F.; Li, C. H.; Li, Q. A dual-responsive liquid crystal elastomer for multi-level encryption and transient information display. *Angew. Chem., Int. Ed.* **2023**, *62*, e202313728.
[24] Choi, J.; Choi, Y.; Lee, J. H.; Kim, M. C.; Park, S.; Hyun, K.; Lee, K. M.; Yoon, T. H.; Ahn, S. K. Direct-ink-written cholesteric liquid crystal elastomer with programmable mechanochromic response. *Adv. Funct. Mater.* **2024**, *34*, 2310658.
[25] Chen, G. C.; Jin, B. J.; Shi, Y. P.; Zhao, Q.; Shen, Y. Q.; Xie, T. Rapidly and repeatedly reprogrammable liquid crystalline elastomer via a shape memory mechanism. *Adv. Mater.* **2022**, *34*, 2201679.
[26] Hussain, S.; Park, S. Y. Photonic cholesteric liquid-crystal elastomers with reprogrammable helical pitch and handedness. *ACS Appl. Mater. Interfaces* **2021**, *13*, 59275–59287.
[27] Herbert, K. M.; Fowler, H. E.; McCracken, J. M.; Schlafmann, K. R.; Koch, J. A.; White, T. J. Synthesis and alignment of liquid crystalline elastomers. *Nat. Rev. Mater.* **2021**, *7*, 23–38.
[28] Chen, G. N.; Wei, W.; Li, S.; Zhou, X. P.; Li, Z. A.; Peng, H. Y.; Xie, X. L. Liquid crystal-assisted manufacturing of flexible holographic polymer nanocomposites for high-security level anticounterfeiting. *Mater. Chem. Front.* **2022**, *6*, 3531–3542.
[29] Li, K.; Wang, J. W.; Cai, W. F.; He, H. L.; Cen, M. J.; Liu, J. X.; Luo, D.; Mu, Q. Q.; Gérard, D.; Liu, Y. J. Electrically switchable, polarization-sensitive encryption based on aluminum nanoaperture arrays integrated with polymer-dispersed liquid crystals. *Nano Lett.* **2021**, *21*, 7183–7190.
[30] Lu, Y. F.; Yang, D. L.; Gao, H.; Du, X.; Zhao, Y. Z.; Wang, D.; He, Z. M.; Miao, Z. C.; Cao, H.; Yang, Z. et al. Enhanced electro-optical properties of polymer-dispersed liquid crystals co-doped with fluorescent molecules and nanoparticles for multifunctional applications. *Chem. Eng. J.* **2024**, *485*, 149654.
[31] Chu, Y. Q.; Miao, Z. C.; Wang, D. Stepwise driving and multi-transparency of polymer dispersion liquid crystals. *Liq. Cryst.* **2023**, *50*, 222–230.
[32] Bagiński, M.; Tupikowska, M.; González-Rubio, G.; Wójcik, M.; Lewandowski, W. Shaping liquid crystals with gold nanoparticles: Helical assemblies with tunable and hierarchical structures via thin-film cooperative interactions. *Adv. Mater.* **2020**, *32*, 1904581.
[33] Gharbi, M. A.; Manet, S.; Lhermitte, J.; Brown, S.; Milette, J.; Toader, V.; Sutton, M.; Reven, L. Reversible nanoparticle cubic lattices in blue phase liquid crystals. *ACS Nano* **2016**, *10*, 3410–3415.
[34] Grzelak, J.; Żuk, M.; Tupikowska, M.; Lewandowski, W. Modifying thermal switchability of liquid crystalline nanoparticles by alkyl ligands variation. *Nanomaterials* **2018**, *8*, 147.
[35] Zhang, S. M.; Shi, W. X.; Wang, X. Locking volatile organic molecules by subnanometer inorganic nanowire-based organogels. *Science* **2022**, *377*, 100–104.
[36] Ni, B.; Shi, Y. A.; Wang, X. The sub-nanometer scale as a new focus in nanoscience. *Adv. Mater.* **2018**, *30*, 1802031.
[37] Zhang, S. M.; Lu, Q. C.; Yu, B.; Cheng, X. J.; Zhuang, J.; Wang, X. Polyoxometalates facilitating synthesis of subnanometer nanowires. *Adv. Funct. Mater.* **2021**, *31*, 2100703.
[38] Lu, Q. C.; Huang, B. L.; Zhang, Q. H.; Chen, S. M.; Gu, L.; Song, L.; Yang, Y.; Wang, X. Single-crystal inorganic helical architectures induced by asymmetrical defects in sub-nanometric wires. *J. Am. Chem. Soc.* **2021**, *143*, 9858–9865.
[39] Jiang, K. Z.; Zhao, D. D.; Guo, S. J.; Zhang, X.; Zhu, X.; Guo, J.; Lu, G.; Huang, X. Q. Efficient oxygen reduction catalysis by subnanometer Pt alloy nanowires. *Sci. Adv.* **2017**, *3*, e1601705.
[40] Liu, J. L.; Li, Y. Q.; Chen, Z.; Liu, N.; Zheng, L. R.; Shi, W. X.; Wang, X. Polyoxometalate cluster-incorporated high entropy oxide sub-1 nm nanowires. *J. Am. Chem. Soc.* **2022**, *144*, 23191–23197.
[41] Li, M. G.; Zhao, Z. L.; Zhang, W. Y.; Luo, M. C.; Tao, L.; Sun, Y. J.; Xia, Z. H.; Chao, Y. G.; Yin, K.; Zhang, Q. H. et al. Sub-monolayer

YO_x/MoO_x on ultrathin Pt nanowires boosts alcohol oxidation electrocatalysis. *Adv. Mater.* **2021**, *33*, 2103762.

[42] Yuan, F.; Ouyang, C.; Yang, M. Z.; Shi, W. X.; Ren, W. B.; Shen, Y.; Wei, Y.; Deng, X. L.; Wang, X. Regulating the mechanical and optical properties of polymer-based nanocomposites by sub-nanowires. *Angew. Chem., Int. Ed.* **2023**, *62*, e202214571.

[43] Zhang, F. H.; Li, Z.; Wang, X. Mechanically tunable organogels from highly charged polyoxometalate clusters loaded with fluorescent dyes. *Nat. Commun.* **2023**, *14*, 8327.

[44] Liu, Q. D.; Sheng, Z.; Shi, W. X.; Cheng, X. J.; Xu, X. X.; Wang, X. Tuning the chirality evolution in achiral subnanometer systems by judicious control of molecule interactions. *J. Am. Chem. Soc.* **2024**, *146*, 12819–12827.

[45] Liu, Q. D.; Zhang, Q. H.; Shi, W. X.; Hu, H. S.; Zhuang, J.; Wang, X. Self-assembly of polyoxometalate clusters into two-dimensional clusterphene structures featuring hexagonal pores. *Nat. Chem.* **2022**, *14*, 433–440.

[46] Zhang, S. M.; Shi, W. X.; Rong, S. J.; Li, S. Z.; Zhuang, J.; Wang, X. Chirality evolution from sub-1 nanometer nanowires to the macroscopic helical structure. *J. Am. Chem. Soc.* **2020**, *142*, 1375–1381.

[47] He, Z.; Wang, J. L.; Chen, S. M.; Liu, J. W.; Yu, S. H. Self-assembly of nanowires: From dynamic monitoring to precision control. *Acc. Chem. Res.* **2022**, *55*, 1480–1491.

[48] Shi, Y. A.; Shi, W. X.; Zhang, S. M.; Wang, X. Revealing the flexibility of inorganic sub-nanowires by single-molecule force spectroscopy. *CCS Chem.* **2023**, *5*, 2956–2965.

[49] Zhang, S. M.; Lin, H. F.; Yang, H. Z.; Ni, B.; Li, H. Y.; Wang, X. Highly flexible and stretchable nanowire superlattice fibers achieved by spring-like structure of sub-1 nm nanowires. *Adv. Funct. Mater.* **2019**, *29*, 1903477.

[50] Zhang, S. M.; Li, J. X.; Shi, W. X.; Zhang, J. T.; Wang, X. Freestanding scattering polarizer assembled with subnanowires and liquid crystals. *Adv. Funct. Mater.* **2024**, *34*, 2405243.

[51] Liu, H. L.; Gong, Q. H.; Yue, Y. H.; Guo, L.; Wang, X. Sub-1 nm nanowire based superlattice showing high strength and low modulus. *J. Am. Chem. Soc.* **2017**, *139*, 8579–8585.

This is an open access article under the terms of the Creative Commons Attribution 4.0 International License (CC BY 4.0, https://creativecommons.org/licenses/by/4.0/).

© The Author(s) 2025. Published by Tsinghua University Press.